THE JOURNAL OF PHYSICAL CHEMISTRY A

ARTICLE

pubs.acs.org/JPCA

Theoretical Studies on Reactions of the Stabilized H_2COO with HO_2 and the $HO_2\cdots H_2O$ Complex

Bo Long,[*,†,§] Xing-feng Tan,[‡] Zheng-wen Long,[§] Yi-bo Wang,[⊥] Da-sen Ren,[†] and Wei-jun Zhang[#]

[†]College of Computer and Information Engineering, Guizhou University for Nationalities, Guiyang, China 550025

[‡]College of Photo-Electronics, Chongqing University of Posts and Telecommunications, Chongqing, China 400065

[§]Department of Physics and [⊥]Key Laboratory of Guizhou High Performance Computational Chemistry, Department of Chemistry, Guizhou University, Guiyang, China 550025

[#]Laboratory of Environment Spectroscopy, Anhui Institute of Optics and Fine Mechanics, Chinese Academy of Sciences, Hefei, China 230031

Supporting Information

ABSTRACT: The reactions of H_2COO with HO_2 and the $HO_2\cdots H_2O$ complex are studied by employing the high-level quantum chemical calculations with B3LYP and CCSD(T) theoretical methods, the conventional transition-state theory (CTST), and the Rice−Ramsperger−Kassel−Marcus (RRKM) with Eckart tunneling correction. The calculated results show that the proton transfer plus the addition reaction channel (TS1A) is preferable for the reaction of H_2COO with HO_2 because the barriers are −10.8 and 1.6 kcal/mol relative to the free reactants and the prereactive complex, respectively, at the CCSD(T)/6-311++G(3df,2p)//B3LYP/6-311++G(d,p) level of theory. Furthermore, the rate constant via TS1A (2.23×10^{-10} cm^3 $molecule^{-1}$ s^{-1}) combined with the concentrations of the species in the atmosphere demonstrates that the HO_2 radical would be the dominant sink of H_2COO in some areas, where the concentration of water is less than 10^{17} molecules cm^{-3}. In addition, although the single water molecule would lower the activated barrier of TS1A from 1.0 to 0.1 kcal/mol with respect to the respective complexes, the rate constant is lower than that of the reaction of HO_2 with H_2COO.

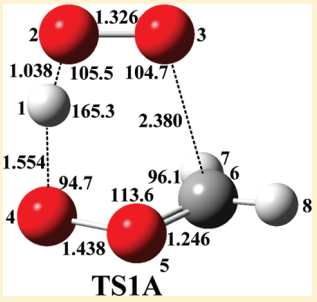

1. INTRODUCTION

The stabilized carbonyl oxides are primarily released into the atmosphere from the ozonolysis of unsaturated volatile organic compounds[1−4] via the Criegee mechanism[5] (Scheme 1). The stabilized carbonyl oxides are crucial in the troposphere because the amount of the unsaturated hydrocarbons emitted into the atmosphere is larger than 630 Tg C/year.[6] Furthermore, ozonolysis is a major sink for unsaturated volatile organic compounds.[7−9] In addition, carboxyl oxides are the key intermediates that contribute to a nonphotochemical source[10−20] of the OH radical and HO_2 radical.[17] Therefore, an accurate knowledge of the loss process of the stabilized carbonyl oxides is of critical importance to fully estimate the environmental impacts of unsaturated volatile organic compounds and carbonyl oxides in the atmosphere.

In the atmosphere, the stabilized carbonyl oxides undergo the bimolecular reactions with other surrounding compounds such as water,[20−26] water dimer,[25] hydroxyl radical,[27] sulfur dioxide,[20,28,29] carbon dioxide,[20] sulfuric acid,[30] aldehydes,[20,31,32] formic acid,[21,33] and ammonia.[34] It is noted that these investigations are mainly based on the quantum chemical calculations because stabilized carbonyl oxides have not been directly detected in the ozonlysis. Very recently, methyl carbonyl oxide has been detected in the reaction of O_2 with dimethyl sulfoxide by Taatjes et al.[35] The bimolecular reactions are of key significance in the atmosphere because the main loss of the stabilized carbonyl oxides affects the level of HO_x in the troposphere and aerosol formation.[36,37] As for the sink of the stabilized carbonyl oxides, the previous theoretical studies[25] have shown that the reaction of carbonyl oxides with water is the primary sink for the H_2COO radical. However, very recently, the theoretical investigation[34] has also indicated that the ammonia with carbonyl oxides reaction may be a sink process in certain regions where the ammonia is in high concentration. On the other hand, the HO_2 radical is one of the biggest oxidants in the atmosphere. Moreover, some reports[38,39] in the literature have proven that the HO_2 radical plays an important role in the radical−radical reaction relative to the atmospheric chemistry. Therefore, exploring the HO_2 radical with the carbonyl oxides is of great interest and necessity.

In this study, we apply ab initio methods, conventional transition-state theory (CTST), and Rice−Ramsperger−Kassel−Marcus (RRKM) to investigate the reaction mechanisms and kinetics of methyl carbonyl oxide with the hydroperoxyl radical and the formed $HO_2\cdots H_2O$ complex. The study is very necessary because HO_2 is an important radical in the atmosphere

Received: January 24, 2011
Revised: May 6, 2011
Published: May 20, 2011

Scheme 1. Formation of the Carbonyl Oxide via the Criegee Mechanism

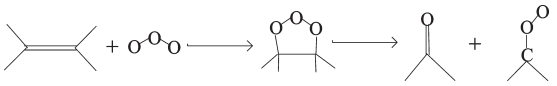

and there are no experimental or theoretical results reported for the reaction of HO_2 with H_2COO. In particular, the reactivity of the formed $HO_2\cdots H_2O$ complex should be taken into account in the atmosphere because 30% of all HO_2[40,41] is in the complex form at 298 K and the $HO_2\cdots H_2O$ complex can accelerate rate constants in the reactions of the HO_2 self-reaction,[42] SO_3,[43] and CF_3OH[44] with the $HO_2\cdots H_2O$ complex.

The investigation involves the hydrogen-bonded complexes formed between $HO_2\cdots H_2O$, HO_2 and H_2COO, the teminal oxygen atom of HO_2 addition to the carbon atom and the hydrogen atom in the HO_2 migration to the terminal oxygen atom of the carbonyl oxide to form $H_2C(OO)OOH$ without and with a water molecule added, and the interconversion between $H_2C(OO)OOH$ conformers, the double proton transfer between H_2COO and HO_2, and the hydrogen abstractions of carbonyl oxides by HO_2 and the hydroperoxyl radical by H_2COO, as schematized in eqs 1−5.

$$H_2COO + HO_2 \rightarrow H_2C(OO)OOH \quad (1)$$

$$H_2COO + HO_2\cdots H_2O \rightarrow H_2C(OO)OOH + H_2O \quad (2)$$

$$H_2COO + HO_2 \rightarrow HCO + OH + HO_2 \quad (3)$$

$$H_2COO + HO_2 \rightarrow HCOO + H_2O_2 \quad (4)$$

$$H_2COO + HO_2 \rightarrow H_2CO + OH + O_2 \quad (5)$$

The goal of this study is to clarify reaction mechanisms to identify the resulting species from the atmospheric oxidation and to evaluate whether the reactions mentioned above are of great importance in the atmospheric chemistry. In addition, the present investigation also provides new insight into the new sink of the stabilized carbonyl oxide in the atmosphere.

2. THEORETICAL METHODS

All electronic structure calculations herein were carried out using the Gaussian03[45] program package. In the first step, the geometries of reactants and complexes formed between HO_2 and H_2COO were optimized by employing the B3LYP hybrid functional method[46] with 6-311G(d, p), 6-311++G(d, p), 6-311++G(3d, 3p), 6-311++G(2df, 2p), 6-311++G(3df, 3pd), aug-cc-pvDz, aug-cc-pvTz, and aug-cc-pvQz basis sets because Cremer et al.[47] have proven that the B3LYP functional with the modest 6-31G(d,p) and 6-311+G(3df,3pd) can reproduce the multireference MR-AQCC/6-311+G(3df,3pd) theoretical results reasonably in the investigation of formation and decomposition of the H_2COO. Test calculation was also performed to check the spin-restricted form (B3LYP) and spin-unrestricted method (uB3LYP) for the reactants and complexes mentioned above. The test results indicate that the energies and vibrational wavenumbers are identical. Therefore, the following computations were finished using the B3LYP functional. The vibrational frequencies were calculated at the corresponding basis sets to confirm the nature of the stationary points and estimate whether the zero-point correction calculations at the different basis sets lead to the different binding energies of the complexes because the tendency is reported on the complex[25] between H_2COO and H_2O. In addition, the basis set superposition error (BSSE) was calculated by employing the counterpoise method by Boys and Bernardi[48] using the B3LYP method at the different basis sets to assess the energetic stability of the complexes better.

In the second step, the geometries and frequencies of the transition states, intermediates, and products were computed by applying the B3LYP method in conjunction with the 6-311++G(d,p) basis set If necessary, the intrinsic reaction coordinate (IRC)[49,50] was employed at the B3LYP/6-311++G-(d, p) level of theory to verify the connectivity between a given transition state with the desired reactants and products. Moreover, to obtain the relative energies reliably and accurately, the single-point calculations were performed using the CCSD(T)[51] methods with respect to the, 6-311++G(3df,2p) basis set at the B3LYP/6-311++G(d,p)-optimized geometries because Nguygen et al.[52] have verified that the single-reference CCSD(T) calculation can appropriately describe the electronic state of the carbonyl oxide via comparison of the CASSCF(12,11) computation at the aug-cc-pvTz basis set. In these computations, the value of the T_1 diagnostic[53] in the CCSD wave function was considered to evaluate the reliability of these computations with respect to a possible multireference feature of the wave function at the stationary points. If the value of the T_1 diagnostic in the CCSD wave functions is larger than 0.044, the CCSD wave functions are thought not to be reliable according to Rienstra-Kiracofe.[54] T_1 diagnostic values of the stationary points except for the TS5, TS6, and TS7 do not exceed the upper limit of 0.044 from Table S1 (Supporting Information), revealing that the CCSD wave function could be reliable.

The bond nature of the complexes in this study was characterized and analyzed in terms of the theory of atoms in molecules (AIM) by Bader[55] executed in AIM2000.[56−58] The analysis was performed over the first-order density matrix, derived from the B3LYP/6-311++G(d, p) level of theory. Finally, the rate constant was evaluated using CTST and RRKM with the Eckart[59] tunneling correction, which was carried out in the TheRate program.[60,61]

3. RESULTS AND DISCUSSION

The optimized geometries of the reactants are provided in Figure 1, and the selected parameters relative to the different basis sets are listed in Table S2 (Supporting Information), which is insensitive to basis sets and is reasonably consistent with the previous results[18−21,27,62−67] published in the literature. The structures of the complexes located in this study are depicted in Figure 1, and the geometrical parameters at the different basis sets are given in Table S3 (Supporting Information), which indicates that the effects of the basis set are also of minor importance. Table S4 (Supporting Information) tells us that the binding energies of C1 with BSSE correction at the different basis sets are in reasonable agreement with one another, revealing again that the basis set effects are not significant. However, it is worth noting that the binding energies of C2 are slightly different from the those of the different basis set in part because the CP correction is not adequate. Test calculations clearly show that the

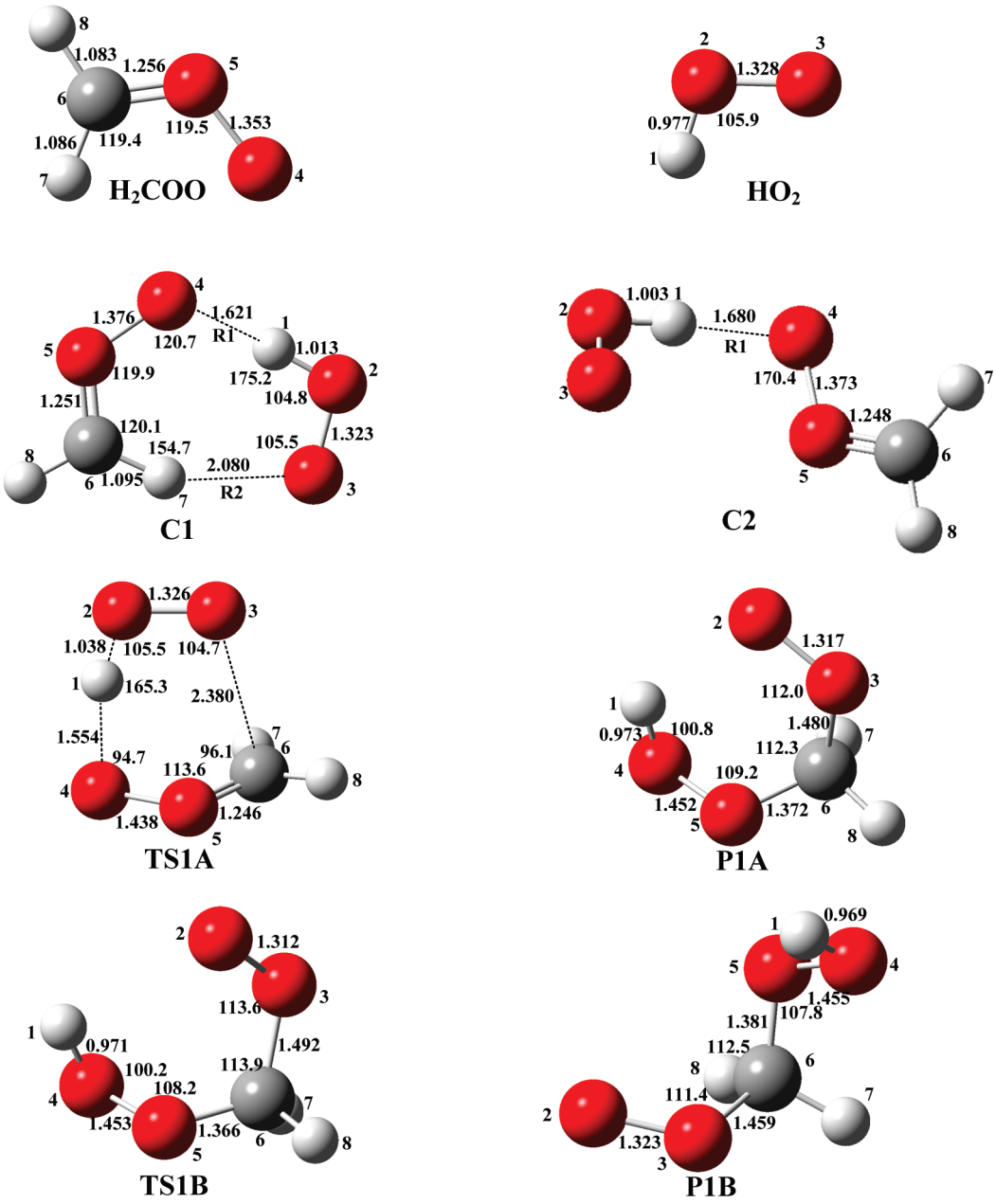

Figure 1. The selected geometrical parameters of the optimized reactants, products, and complexes at the B3LYP/6-311++G(d,p) level of theory (bond distances in angstroms and angles in degrees).

effects of basis sets are not an issue. Therefore, the other stationary points reported herein are computed at the B3LYP/6-311++G(d,p) level of theory.

3.1. Hydrogen Transfer Plus Oxygen Addition Reaction between H_2COO and HO_2. The previous investigation has shown that the dominant sink of the stabilized methyl carbonyl oxide is reaction with water and the water dimer in the atmosphere. The reactions of H_2COO with water and the water dimer are reproduced in order to estimate whether the reactions investigated herein are more efficient for the sink of the H_2COO radical than the corresponding reactions with water and the water dimer. As the reactions of H_2COO with water[20−22,25] and the water dimer[25] have been extensively investigated in the literature, we only take into account the reactions from the energetic point of view. The geometrical structures are provided in Figure S1 (Supporting Information). The binding energy of the $H_2COO\cdots H_2O$ is found to be −6.2 kcal/mol from Table 1, which is slightly different from the corresponding values reported by Anglada[21] (−7.8 kcal/mol) and by Ariya[25] (−5.8 kcal/mol) due to the BSSE correction and zero-point energy correction at the different levels of theory. However, the activated barrier via the TS01 is calculated to be 9.4 kcal/mol relative to the prereactive complex, agreeing well with the reported values of 9.8 kcal/mol by Anglada[21] and 9.5 kcal/mol by Aplincourt.[20] The stabilized energy (−13.3 kcal/mol) of the complex C02 formed between the carbonyl oxide and the water dimer is perfectly consistent with the corresponding energy of −13.3 kcal/mol with BSSE correction by Ariya.[25] It is noted that the energy barrier of the corresponding transition state TS02 is

dx.doi.org/10.1021/jp200729q |J. Phys. Chem. A 2011, 115, 6559–6567

Table 1. Binding, Activated, and Reaction Energies, Enthalpies, and Free Energies for the Reactions of H_2COO with H_2O, the Water Dimer, HO_2, and $HO_2\cdots H_2O$ with Zero-Point Correction Included at 298 K (kcal/mol)

compound	ΔH^a	ΔG^a	ZPE^a	ΔE^a	ΔE^b
$H_2COO + H_2O$	0.0	0.0	32.8	0.0	0.0
C01	−7.2	0.8	34.9	−6.7	−6.2
TS01	0.5	11.8	35.3	2.3	3.2
$H_2C(OH)COOH$	−40.5	−30.0	37.8	−39.1	−42.4
$H_2COO + H_2O + H_2O$	0.0	0.0	46.2	0.0	0.0
C02	−16.5	1.7	51.2	−15.1	−13.3
TS02	−15.1	6.5	51.0	−12.2	−9.7
$H_2C(OH)COOH + H_2O$	−40.5	−30.0	51.2	−39.1	−42.4
$H_2COO + HO_2$	0.0	0.0	28.3	0.0	0.0
C1	−12.6	−2.8	30.1	−12.2	−11.8
TS1A	−11.4	0.22	29.8	−10.4	−10.8
P1A	−44.3	−32.7	32.4	−43.3	−47.6
TS1B	−43.6	−31.1	32.1	−42.2	−46.2
P1B	−44.5	−33.3	32.2	−43.6	−47.8
TS2	−4.7	6.0	26.6	−3.8	−2.3
C20	−3.9	6.4	29.4	−3.3	−3.7
$HCO + OH + HO_2$	−11.3	−22.2	26.8	−13.1	−10.9
C2	−10.5	−2.0	29.9	−10.3	−9.7
TS3	−8.7	1.6	26.7	−8.1	−0.4
$HCHO + OH + O_2$	−49.0	−52.3	24.3	−50.5	−50.4
$H_2COO + H_2O + HO_2$	0.0	0.0	41.6	0.0	0.0
C3	−22.4	−2.7	45.4	−21.1	−18.4
TS4	−24.1	−2.2	44.6	−21.9	−18.3
$P1A + H_2O$	−44.3	−32.7	45.8	−43.3	−47.6
$H_2COO + HO_2$	0.0	0.0	28.3	0.0	0.0
TS5	21.1	29.9	25.3	21.3	30.7
TS6	21.3	29.8	25.3	21.4	30.8
TS7	21.8	31.0	26.0	22.1	38.3

[a] The values are computed at the B3LYP/6-311++G(d,p) level of theory. [b] The values are obtained at the CCSD(T)/6-311++G(3df,2p)//B3LYP/6-311++G(d,p) level of theory plus BSSE at the B3LYP/6-311++G(3df,2p) level of theory.

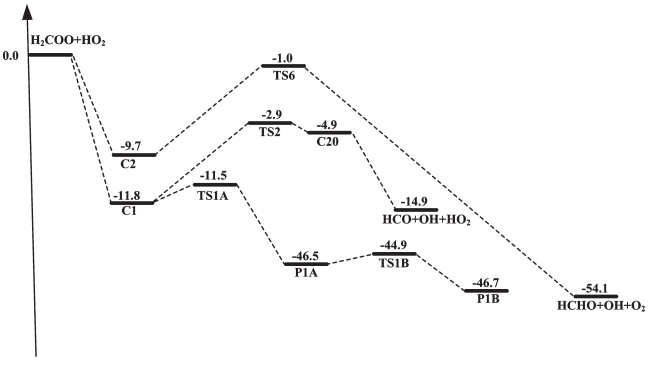

Figure 2. The calculated potential energy profile for the reaction $H_2COO + HO_2$ at the CCSD(T)/6-311++G(3df,2p)//B3LYP/6-311++G(d,p) level of theory (in kcal/mol).

computed to be 3.6 kcal/mol, which is lower than the reported value of 6.6 kcal/mol by Ariya.[25]

Table 2. Topological Properties of the Bond Critical Points of the $H_2COO_4\cdots HO_2$ and $H_2COO_4\cdots HO_2\cdots H_2O$ Complexes at the B3LYP/6-311++G(d,p) Level of Theory

compound	bond/ring	r^a	ρ (au)^b	$\Delta^2\rho$ (au)^c	G (au)^d	V (au)^e	H (au)^f
C1	H1O4	1.621	0.0539	0.1352	0.0424	−0.0510	−0.0086
	O3H7	2.080	0.0217	0.0684	0.0153	−0.0135	0.0018
	(3,1)	–	0.0078	0.0344	0.0074	−0.0062	0.0012
C2	H1O4	1.680	0.0488	0.1364	0.0397	−0.0453	−0.0056
C3	O4H9	1.611	0.0577	0.1444	0.0468	−0.0575	−0.0107
	H1O10	1.527	0.0705	0.1556	0.0570	−0.0751	−0.0181
	O3C6	2.241	0.0270	0.0816	0.0193	−0.0182	0.0011
	(3,1)		0.0034	0.0172	0.0034	−0.0025	0.0009

[a] The distance of hydrogen bonding. [b] Electronic charge density at the critical point. [c] Laplacian of the electron density at the bond critical point. [d] Kinetic electron density at the bond critical point. [e] Potential electron energy density at the bond critical point. [f] Total electron energy density at the bond critical point.

The reaction begins with the formation of the precomplex C1 and proceeds through the transition state TS1A to lead to form the intermediate P1A in Figure 1. The calculated potential profile is given in Figure 2, which depicts the reaction process. Due to the HO_2 radical with the open-shell structure, we take into account the spin doublet state and quartet state for the complex located herein. However, the complex at the spin doublet state can be stabilized. The complex C1 is a planar seven-member ring structure with double hydrogen bonds similar to the complexes formed between formic acid,[68,69] nitric acid,[70] and HO_2. From Table 1, the calculated binding energy of the complex C1 is −11.8 kcal/mol at the CCSD(t)/6-311++G(3df,2p)//B3LYP/6-311++G(d,p) level of theory, which is about 4.0 kcal/mol lower than that of the complex between the carbonyl oxide and water.[21,25] In addition, from Table 1, a negative free energy of $\Delta G = -2.8$ kcal/mol at 298 K indicates that the formation of the complex C1 is thermodynamically driven. From a geometrical point of view, the H1O2 and C6H7 bonds in the complex C1 are stretched by 3.6 and 0.8% with respect to the free reactants, respectively, while the H1O4 bond distance of 1.621 Å is 0.432 Å shorter than that of the O3C7 bond with the distance of 2.080 Å, which indicates that the O4···H1O2 bond strength is stronger than that of the corresponding C6H7···O3. Additionally, the quantum theory of atoms-in-molecules is a useful tool to analyze the bonding natures as reported by Bader.[55] Moreover, according to the AIM theory, Koch and Propelier[71] gives two quantitative criteria to characterize the hydrogen bond interactions: the electron density (ρ_{bcp}) and the Laplacian of the electron density ($\Delta^2\rho_{bcp}$) at the bond critical points in the ranges of 0.02−0.04 and 0.024−0.139 au, respectively. It has also pointed out[55] that the Laplacian of the electron density ($\Delta^2\rho_{bcp}$) is positive and the total electron energy density (H_{bcp}) is negative, unraveling that the hydrogen-bonded interactions are partially covalent and partially electrostatic in nature, whereas the total electron energy density is positive, unveiling that the hydrogen bond has only electrostatic interactions. From Table 2, it is noted that the ρ_{H1O4} = 0.0539 au extends the upper limit of the criteria[71] and the H_{H1O4} is −0.0086 au, reflecting the strong hydrogen bond interaction.

The transition state (TS1A) involves the transfer of the hydrogen in the HO_2 radical to the terminal oxygen of the carbonyl oxide, with the simultaneous terminal oxygen addition

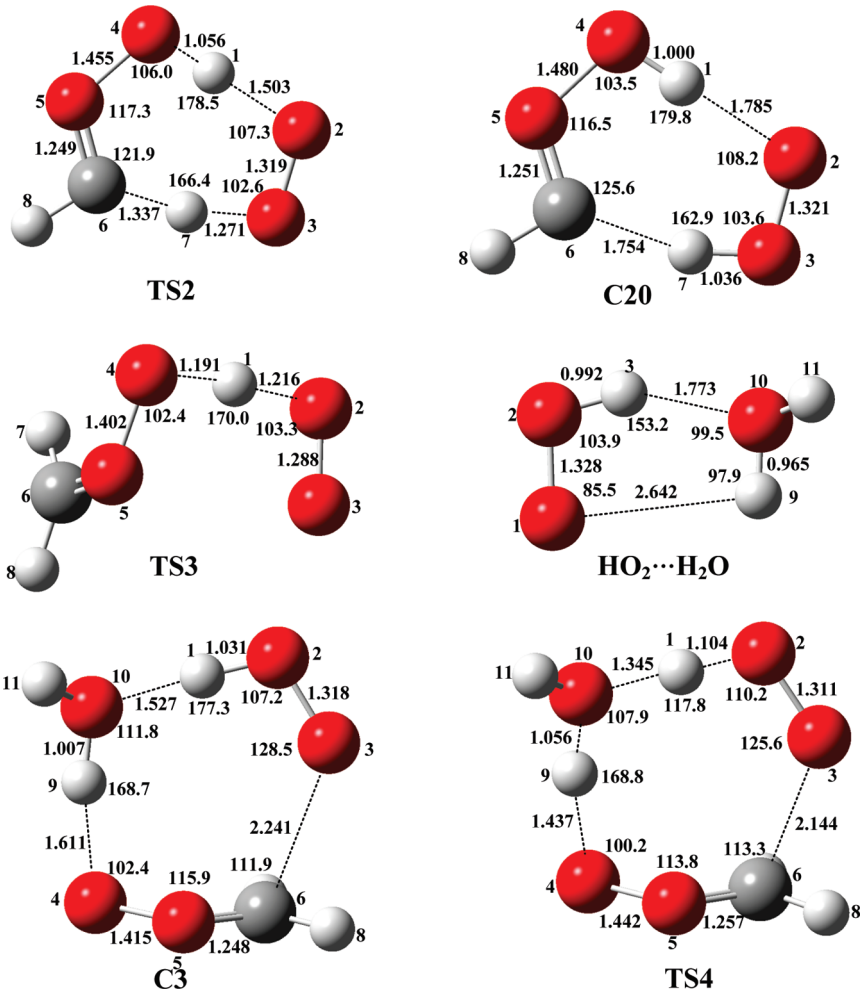

Figure 3. The geometrical structures of the optimized transition state, intermediates, and complexes at the B3LYP/6-311++G(d,p) level of theory (bond distances in angstroms and angles in degrees).

to the central carbon atom in the carbonyl oxide and an electron transfer between the two oxygen atoms of the HO_2 radical, which is similar to the reactions of SO_3[43] and HCHO[72,73] with the HO_2 radical, called the proton-transfer coupled electron transfer. The activated energy is calculated to be 1.0 kcal/mol relative to the corresponding precomplex C1, which is about 8.0 and 5.0 kcal/mol lower than those of the reactions of the carbonyl oxide with water[20−22,25] and the water dimer,[25] indicating that the reaction via TS1A is energetically favored. Additionally, the atom spin population in TS1A was calculated using the AIM theory as presented in Figure S1 (Supporting Information). As a result, the spin population in TS1A is focused on the O2 and O3, and the spin populations of O4 and the transferred H1 are negative and partly responsible for the lower energy barrier because the triplet repulsion is negligible, as reported in the literature.[73] From the geometrical point of view, in TS1A, the dihedral angles ∠H1O2O3C6 and ∠H1O2O3O4 are −2.9 and −1.4°, respectively, reflecting that the five atoms (H1O2O3O4C6) approximately lay in the same plane. The O4O5 bond is stretched to 1.438 Å in TS1A from 1.353 Å in the H_2COO radical, and it is further lengthened to 1.452 Å as the O4H1 atoms approach the formation of the H1O4 single bond in the product (P1A), which is similar to the reaction of $H_2O + H_2COO$ radical.[20−22,25] The intermediate $H_2C(OO)OOH$ corresponding to two conformers (P1A and P1B) is connected by the transition state TS1B with a computed barrier of about 1.4 kcal/mol. The calculated results show that the conformer P1B is more stable than the P1A by 0.2 kcal/mol.

Regarding the fate of the intermediate $H_2C(OO)OOH$ in the atmosphere, it is reacted with NO to produce NO_2 and the $H_2C(O)OOH$ alkoxy radical. Furthermore, the $H_2C(O)OOH$ radical undergoes hydrogen transfer from O4 to O3, yielding the peroxy radical $H_2C(OO)OH$, as proposed by Su[74] and reported in the literature.[72,73,75] The peroxy radical $H_2C(OO)OH$ goes through unimolecular decomposition to produce HCHO + HO_2, which has been reported in the literature.[72,75] The conclusion is that the reaction of carbonyl oxide with HO_2 yields the HCHO and the HO_2 radical, and thus, the HO_2 radical is regarded as a catalyst in the reaction of carbonyl oxide with HO_2.

3.2. Double Proton Transfer. The reaction is a very complex mechanism because of the formation of the prereactive complex C1 prior to the transition state TS2 (in Figure 3) and the postcomplex C20 similar to the reactions of carbonyl oxide with OH[72] and H_2O[21,22] as catalysts. From Table 1, the barrier is computed to be about 9.5 and −2.3 kcal/mol with respect to the precomplex C1 and the reactants, respectively, indicating that the HO_2 exerts the strongest catalytic effect because the barrier is 34.9, 8.5, and 13.0 kcal/mol lower than those of the corresponding

dx.doi.org/10.1021/jp200729q |J. Phys. Chem. A 2011, 115, 6559–6567

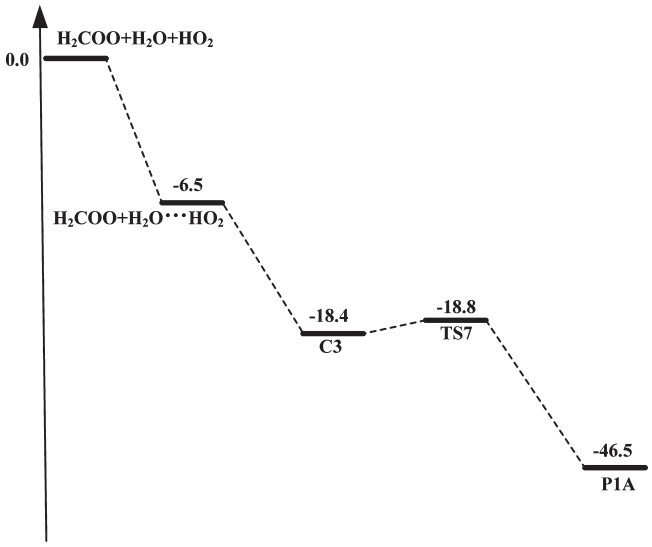

Figure 4. The calculated potential energy profile for the H_2COO reaction with $HO_2\cdots H_2O$ at the CCSD(T)/6-311++G(3df,2p)//B3LYP/6-311++G(d,p) level of theory (in kcal/mol).

reaction ($H_2COO \rightarrow HCO + OH$) with respect to the reactant,[76] the reaction ($H_2COO + H_2O \rightarrow HCO + OH + H_2O$) relative to the prereactive complex,[22] and the reaction ($H_2COO + OH \rightarrow HCO + 2OH$) relative to the prereactive complex,[27] respectively. However, the energy barrier is 8.5 kcal/mol higher than that of TS1A, showing that the reaction pathway is minor for the loss of the stabilized methyl carbonyl oxide. The intermediate complex C20 is a planar seven-ring member structure involving double hydrogen bonds with a binding energy of −3.7 kcal/mol.

3.3. Hydrogen Abstraction. The hydrogen atom of HO_2 abstracted by H_2COO occurs via the prereactive complex C2 and the corresponding transition state TS3 similar to the process of the hydrogen atom of HO_2 abstracted by ozone.[77] The complex C2 is stabilized by the interaction between the terminal oxygen atom of carbonyl oxide and the hydrogen atom of HO_2, resulting in the formation of the single hydrogen bond complex. Compared with the complex C1, the angle ∠O4H1O2 in C2 is 5.9° smaller than the counterpart in the complex C1. Additionally, the O4···H1 in complex C1 is 0.059 Å shorter than that of the complex C2. Therefore, the geometrical parameters show that the interaction of O4···H1O2 in C1 is stronger than that of C2. It is worth noting that although the binding energy of C2 is found to be −9.7 kcal/mol and the topological analysis also demonstrates that the interaction between H1 and O4 in C2 is partially covalent in nature, the topological properties also show that the strength between H1 and O4 in C1 is stronger than the corresponding interaction in C2. This may lead to the activated barrier via TS3 being higher than the TS1A. The energy barrier is calculated to be −0.4 and 9.3 kcal/mol with respect to the separate reactants and the prereactant, respectively, which is higher than the value of TS1A by 10.4 kcal/mol relative to the reactants. Therefore, the elementary process via TS3 is of no importance for the sink of methyl carbonyl oxide. In addition, the HO_2 radical extracts the hydrogen of the carbonyl oxide via the transition states TS5, TS6, and TS7 in Figure S1 (Supporting Information). Table 1 tells us that the barriers are in the range of 30.7−38.0 kcal/mol, showing that these processes unlikely take place in the atmosphere. Thus, the reaction channels are not contributed to the loss of the stabilized methyl carbonyl oxide.

3.4. Proton Transfer Plus Oxygen Addition Reaction between H_2COO and the $HO_2\cdots H_2O$ Complex. Herein, the reaction taking place between the carbonyl oxide and the formed $HO_2\cdots H_2O$ complex is considered to judge whether the reaction is more feasible than the naked reaction $H_2COO + HO_2$. Furthermore, the proton transfer plus oxygen addition reaction between H_2COO and the formed $HO_2\cdots H_2O$ complex is taken into account because the calculated results have proven that the hydrogen transfer plus the oxygen addition reaction between H_2COO and HO_2 is more preferable than other reaction channels between H_2COO and HO_2. In addition, the reaction of $H_2COO\cdots H_2O$ with HO_2 is also considered to examine whether this could be one of the exit channels of the reaction. However, the corresponding stationary points are not located. Therefore, the results reflect that this is not the exit channel for the reaction of $H_2COO + HO_2$ with the single water molecule.

The reaction starts with the precomplex C3 before the transition state TS4 and the products $H_2C(OO)OOH$ and H_2O, which is clearly depicted in the calculated potential profile in Figure 4. In the elementary process, the water molecule is released and thus acts as a catalyst. The C3 is an eight-member ring structure including two hydrogen bonds between O4 and H9 and H1 and O10 and a weak bond interaction between the terminal oxygen in the HO_2 and the center carbon in the H_2COO. The O4···H9, O10···H1, and O3···C6 bond distances are 1.611, 1.527, and 2.241 Å, respectively, reflecting that the bond strength between O10 and H1 is stronger than those of the other two bonds, whereas the O3···C6 interaction is weakest in the three bonds. The topological analysis of the wave function ($\rho_{O4H9} = 0.0577$ au, $\Delta^2\rho_{O4H9} = 0.1444$ au, $\rho_{O10H1} = 0.0705$ au, $\Delta^2\rho_{O10H1} = 0.1556$ au, $\rho_{C6O3} = 0.0270$ au, and $\Delta^2\rho_{C6O3} = 0.0816$ au) at the bond critical points also indicates that the O10H1 interaction is strongest in the three bonds. It is pointed out the strong interaction between H1 and O10 leads to the hydrogen transfer between O2 and O4 with the low-energy barrier. The binding energy is found to be about −18.4 kcal/mol, which is 6.6 and 4.0 kcal/mol lower than the counterparts $H_2COO\cdots HO_2$ and $H_2COO\cdots 2H_2O$,[25] respectively.

The transition state TS4 is an eight-member ring structure involving the double proton transfers of H1 of the HO_2 to the O10 in the water and of H9 in the H_2O to the terminal oxygen in the H_2COO and the O3 atom addition to the C6 atom of the H_2COO. From an electronic point of view, from Figure S1 (Supporting Information), the atom spin population is centered on the O2 and O3 atoms with positive value, whereas the spin populations of H1 and O10 are negative, leading to being free of the triplet repulsion similar to the transition state TS1A. The activated energy is lower than the TS1A by 0.1 kcal/mol relative to the respective precomplex. The low-energy barrier shows that the water molecule plays a strong catalytic role in the reaction of H_2COO and HO_2.

3.5. Kinetics and the Potential Application Relevant to Atmospheric Chemistry. The rate constant is reported herein to estimate whether the reactions of H_2COO with HO_2 and the $HO_2\cdots H_2O$ complex can compete well with the reactions of $H_2COO + H_2O$ and $H_2COO + H_2O\cdots H_2O$ because the major removal of H_2COO in the atmosphere was previously considered to be the reactions of H_2COO with water and the water dimer.[25] According to the results discussed above, main

Table 3. Rate Constant (k, cm^3 molecule^{-1} s^{-1}) for the Individual Reaction Pathway in the Temperature Range of 200−298 K

reaction	200 K	220 K	240 K	260 K	280 K	298 K
k_{TS01}	1.31×10^{-17}	2.15×10^{-17}	3.27×10^{-17}	4.67×10^{-17}	6.37×10^{-17}	8.15×10^{-17}
k_{TS02}	6.82×10^{-9}	1.12×10^{-9}	2.47×10^{-10}	6.82×10^{-11}	2.25×10^{-11}	9.30×10^{-12}
k_{TS02}	3.21×10^{-12}	2.53×10^{-13}	3.05×10^{-14}	5.11×10^{-15}	1.11×10^{-15}	3.36×10^{-16}
k_{TS1A}	1.83×10^{-10}	1.92×10^{-10}	2.00×10^{-10}	2.08×10^{-10}	2.16×10^{-10}	2.23×10^{-10}
k_{TS4}	1.80×10^{-10}	1.89×10^{-10}	1.97×10^{-10}	2.05×10^{-10}	2.13×10^{-10}	2.19×10^{-10}

reaction channels of the reactions $H_2COO + HO_2$ and $H_2COO + HO_2\cdots H_2O$ are TS1A and TS4, and thus, the corresponding rate constants are computed. Becuase the reaction begins with the formation of the prereactive complex before the transition sate, the reaction process is depicted by the eq 6.

$$\begin{matrix} H_2COO + HO_2 \\ H_2COO + HO_2\cdots H_2O \end{matrix} \overset{k_1}{\underset{k_{-1}}{\rightleftarrows}} \text{Prereactive complex} \xrightarrow{k_2} \text{Product} \tag{6}$$

By assuming that the prereactive complex is in equilibrium with the reactants and the steady-state conditions, the overall rate constant is obtained as

$$k = \frac{k_1 k_2}{k_{-1} + k_2} \tag{7}$$

If $k_2 \ll k_{-1}$, the rate constant is expressed as

$$k = \frac{k_1}{k_{-1} + k_2} k_2 = K_{eq} k_2 \tag{8}$$

where the K_{eq} and k_2 represent the equilibrium constant of the first step and the rate constant of the second step in eq 6, respectively. If the k_2 is much bigger than k_{-1}, the overall rate constant is approximately equal to k_1, which is derived from the hard-sphere collision theory. Finally, the overall rate constant is estimated according to eq 7. The k_{-1} is calculated from the equilibrium constant K_{eq} and k_1. The k_2 is the rate constant of the second step calculated in the TheRate with Eckart tunneling correction. We have utilized the method to study the reaction of sulfuric acid[77] with OH in the presence of water. The detailed results are shown in Tables S5 and S6 (Supporting Information), and the computational rate constants indicate that the values that are obtained using transition-state theory and RRKM are in close agreement with each other. Thus, the rate constants listed in Table 3 are estimated employing the transition-state theory. In addition, the rate constant for the reaction of H_2COO with the water dimer is calculated using the pseudo-second-order approximation as proposed by Alvarez-Idaboy et al.[78]

As far as we know, the kinetics[79−82] of the reaction of carbonyl oxide with water is inconsistent and differs in the range of 1×10^{-19}−1×10^{-15} cm^3 molecule^{-1} s^{-1}. The rate constant of k_{TS01} is 8.15×10^{-17} cm^3 molecule^{-1} s^{-1}, which is in the range of experimental results and is slightly different from the previous calculation by Ariya[25] because the calculated energy barrier here is about 1.0 kcal/mol lower than the value reported by Ariya.[25] However, as for the reaction of H_2COO with the water dimer, the rate constant is calculated by using two different methods because Alvarez-Idaboy et al.[78] have shown that extrapolating results obtained in chamber experiments is not always likely for the bimolecular processes that produce a product at atmospheric concentrations. The k_{TS02} and k'_{TS02} are obtained using the pseudo-first- and -second-order approximations, respectively. The k_{TS02} agrees reasonably with the computed value by Ariya.[25] It is noted that the k'_{TS02} is in the range of 3.05×10^{-14}−3.36×10^{-16} cm^3 molecule^{-1} s^{-1} with the temperature range of 240−298 K. The results indicate that the experimental data[79−82] of the reaction of H_2COO with water are largely changed mainly because it involves the reaction of H_2COO with the water dimer, which is very similar to the process of the reaction[83−87] of SO_3 with the water dimer responsible for the formation of the sulfuric acid. From Table 3, the calculated rate constants show that the reaction of H_2COO with HO_2 via TS1A is dominant. The rate constant of TS1A is computed to be 2.23×10^{-10} cm^3 molecule^{-1} s^{-1} at 298 K. If the reaction via TS1A could play an important role in the sink for the stabilized H_2COO in the atmosphere, the concentration of HO_2 is 10^{-7} and 10^{-2} greater than the concentrations of the water molecule and the water dimer, respectively. Moreover, the upper limit concentrations[88−90] of H_2O and the water dimer are 3.97×10^{17} and 2.69×10^{14} molecules cm^{-3} at 50% relative humidity and at 298 K, while the highest concentration of HO_2 is 2.00×10^9 molecules cm^{-3} at 298 K. In addition, the lifetime of H_2COO is about 0.03 s with the water concentration of 3.97×10^{17} molecules cm^{-3}, whereas it is about 2.24 s with the HO_2 concentration of 2.00×10^9 molecules cm^{-3} at 298 K. Therefore, the reaction of H_2COO with HO_2 is not dominant in the atmosphere, where the concentration of water is up to 10^{17} molecules cm^{-3}. However, in the upper atmosphere[91] of above 35 km, the concentration of water is very low. The reaction $H_2COO + HO_2$ may play an important role in the sink of H_2COO. In addition, the rate of the reaction of H_2COO with HO_2 is 10^4 times faster than that of $NH_3 + H_2COO$ reaction,[34] whereas the concentration of HO_2 is 10^{-3} greater than that of NH_3. Therefore, the reaction of $H_2COO + HO_2$ is more important than the $NH_3 + H_2COO$. Furthermore, regarding the reaction of H_2COO with the $HO_2\cdots H_2O$ complex, the concentration of the $HO_2\cdots H_2O$ complex is determined by the water molecule. The typical value of the $HO_2\cdots H_2O$ complex is about 10^8 molecules cm^{-3}, which would not compete well with the single water molecule and the water dimer. Additionally, it is pointed out that the investigation of the reaction of methyl carbonyl oxide with HO_2 needs to be further studied experimentally because the results reported herein are on the basis of theoretical calculations. Although it is of great difficulty to detect the carbonyl oxide in the atmosphere because, until recently, the carbonyl oxide only has been detected in the reaction of O_2 with dimethyl sulfoxide (DMSO),[35] the role of the HO_2 radical in the ozonolysis of unsaturated hydrocarbons is indirectly measured according to the theoretical results.

4. CONCLUSIONS

We have investigated the reactions of H_2COO with HO_2 and the $HO_2\cdots H_2O$ complex utilizing B3LYP and CCSD(T)

theoretical approaches for the first time. To obtain the calculated results reliably, test calculations were first executed to check whether the geometrical structures and binding energies of the complexes between HO_2 and H_2COO are affected by the different levels of theory. The calculated results clearly demonstrate that the selected methods can describe the reaction system reliably. The two strong hydrogen-bonded complexes formed between H_2COO and HO_2, whose binding energies are computed to be −12.4 and −10.1 kcal/mol at the CCSD(T)/6-311++G(3df,2p)//B3LYP/6-311++G(d,p) level of theory. In addition, the proton transfer plus oxygen addition in the reaction of HO_2 and H_2COO is the predominant reaction pathway, whereas the double proton transfer and the hydrogen abstraction of HO_2 by H_2COO are minor because the barrier via TS1A is a very small barrier with values of 1.0 and −10.8 kcal/mol relevant to the prereactive complex and the free reactants, respectively. It is interesting that the reaction by TS1A is finally responsible for the formation of HCHO and HO_2. The H_2COO reaction with HO_2 in the atmosphere is significant in some areas, where the concentration of water is less than 10^{17} molecules cm^{-3}. In addition, the accurate rate constant of H_2COO with H_2O is further studied, which is of great necessity because the uncertainty of the rate constant leads to the difficulty in comparing what is the dominant species responsible for the loss of the carbonyl oxides. The rate constant of the reaction of H_2COO with the water dimer is re-estimated using the pseudo-second-order kinetic computation, revealing that the experimental data of the reaction $H_2COO + H_2O$ is not consistent due to the involvement of the reaction of carbonyl oxide with the water dimer. Finally, the NO with H_2COO reaction is also provided in Table S7 and Figure S2 (Supporting Information), unraveling that the reaction is not kinetically favorable.

■ ASSOCIATED CONTENT

Supporting Information. Tables S1−S6 contain geometrical parameters for reactants and complexes, the binding energies of the complexes, and the detailed rate constants. Table S7 reports the rate constant of the reaction $H_2COO + NO$. Figure S1 involves the spin populations of the TS1A and TS4 and the geometrical structures for the reactions of H_2COO with water and the water dimer. Figure S2 represents the potential energy profile for the reaction $H_2COO + NO$. This material is available free of charge via the Internet at http://pubs.acs.org.

■ AUTHOR INFORMATION

Corresponding Author
*E-mail: wwwltcommon@sina.com.

■ ACKNOWLEDGMENT

This research has been supported by Guizhou University for Nationalities (2010). The authors thank anonymous referees for providing the valuable comments

■ REFERENCES

(1) Hasson, A. S.; Orzechowska, G.; Paulson, S. E. *J. Geophys. Res., Atmos.* **2001**, *106*, 131.
(2) Hasson, A. S.; Ho, A. W.; Kuwata, K. T.; Paulson, S. E. *J. Geophys. Res., Atmos.* **2001**, *106*, 143.
(3) Drozd, G. T.; Donahue, N. M. *J. Phys. Chem. A* **2011**, *115*, 4381.
(4) Drozd, G. T.; Kroll, J.; Donahue, N. M. *J. Phys. Chem. A* **2011**, *115*, 161.
(5) Criegee, R. *Angew. Chem., Int. Ed. Engl.* **1975**, *14*, 745.
(6) Finlayson-Pitts, B. J.; Pitts, J. N. *Chemistry of the Upper and Lower Atmosphere*; Academic Press: San Diego, CA, 2000.
(7) Atkinson, R.; Carter, W. P. L. *Chem. Rev.* **1984**, *84*, 437.
(8) Grosjean, D. *Environ. Sci. Technol.* **1990**, *24* (9), 1428.
(9) Johnson, D.; Marston, G. *Chem. Soc. Rev.* **2008**, *37* (4), 699.
(10) Paulson, S. E.; Orlando, J. J. *Geophys. Res. Lett.* **1996**, *23*, 3727.
(11) Kroll, J. H.; Hanisco, T. F.; Donahue, N. M.; Demerjian, K. L.; Anderson, J. G. *Geophys. Res. Lett.* **2001**, *28*, 3863.
(12) Hu, J.; Stedman, D. H. *Environ. Sci. Technol.* **1995**, *29*, 1655.
(13) Heard, D. E.; Pilling, M. J. *Chem. Rev.* **2003**, *103*, 5163.
(14) Atkinson, R.; Aschmann, S. M. *Environ. Sci. Technol.* **1993**, *27*, 1357.
(15) Carlo, P. D.; Brune, W. H.; Martinez, M.; Harder, H.; Lesher, R.; Ren, X.; Thornberry, T.; Carroll, M. A.; Young, V.; Shepson, P. B.; Riemer, D.; Apel, E.; Campbell, C. *Science* **2004**, *304*, 722.
(16) Gutbrod, R.; Kraka, E.; Schindler, R. N.; Cremer, D. *J. Am. Chem. Soc.* **1997**, *119*, 7330.
(17) Mihelcic, D.; Heitlinger, M.; Kley, D.; Müsgen, P.; Volz-Thomas, A. *Chem. Phys. Lett.* **1999**, *301*, 559.
(18) Anglada, J. M.; Bofill, J. M.; Olivella, S.; Sole, A. *J. Am. Chem. Soc.* **1996**, *118* (19), 4636.
(19) Anglada, J. M.; Crehuet, R.; Bofill, J. M. *Chem.— Eur. J.* **1999**, *5* (6), 1809.
(20) Aplincourt, P.; Ruiz-Lopez, M. F. *J. Am. Chem. Soc.* **2000**, *122* (37), 8990.
(21) Crehuet, R.; Anglada, J. M.; Bofill, J. M. *Chem.—Eur. J.* **2001**, *7* (10), 2227.
(22) Anglada, J. M.; Aplincourt, P.; Bofill, J. M.; Cremer, D. *ChemPhysChem* **2002**, *2*, 215.
(23) Hasson, A. S.; Chung, M. Y.; Kuwata, K. T.; Converse, A. D.; Krohn, D.; Paulson, S. E. *J. Phys. Chem. A* **2003**, *107* (32), 6176.
(24) Kroll, J. H.; Sahay, S. R.; Anderson, J. G.; Demerjian, K. L.; Donahue, N. M. *J. Phys. Chem. A* **2001**, *105* (18), 4446.
(25) Ryzhkov, A. B.; Ariya, P. A. *Phys. Chem. Chem. Phys.* **2004**, *6* (21), 5042.
(26) Kuwata, K. T.; Hermes, M. R.; Carlson, M. J.; Zogg, C. K. *J. Phys. Chem. A* **2010**, *114*, 9192.
(27) Mansergas, A.; Anglada, J. M. *J. Phys. Chem. A* **2006**, *110* (11), 4001.
(28) Hatakeyama, S.; Kobayashi, H.; Akimoto, H. *J. Phys. Chem.* **1984**, *88* (20), 4736.
(29) Jiang, L.; Xu, Y. S.; Ding, A. Z. *J. Phys. Chem. A* **2010**, *114*, 12452.
(30) Kurtén, T.; Bonn, B.; Vehkamaki, H.; Kulmala, M. *J. Phys. Chem. A* **2007**, *111* (17), 3394.
(31) Neeb, P.; Horie, O.; Moortgat, G. K. *J. Phys. Chem. A* **1998**, *102* (34), 6778.
(32) Tobias, H. J.; Ziemann, P. J. *J. Phys.Chem. A* **2001**, *105* (25), 6129.
(33) Long, B.; Cheng, J. R.; Tan, X. F.; Zhang, W. J. *J. Mol. Struct: THEOCHEM* **2009**, *916*, 159.
(34) Jørgensen, S.; Gross, A. *J. Phys. Chem. A* **2009**, *113*, 10284.
(35) Taatjes, C. A.; Meloni, G.; Selby, T. M.; Trevitt, A. J.; Osborn, D. L.; Percival, C. J.; Shallcross, D. E. *J. Am. Chem. Soc.* **2008**, *130* (36), 11883.
(36) Lee, S.; Kamens, R. M. *Atmos. Environ.* **2005**, *39* (36), 6822.
(37) Heard, D. E.; Carpenter, L. J.; Creasey, D. J.; Hopkins, J. R.; Lee, J. D.; Lewis, A. C.; Pilling, M. J.; Seakins, P. W.; Carslaw, N. *Geophys. Res. Lett.* **2004**, *31*, L18112.
(38) Anglada, J. M.; Olivella, S.; Solé, A. *J. Phys. Chem. A* **2007**, *111*, 1695.
(39) Anglada, J. M.; Olivella, S.; Solé, A. *J. Phys. Chem. A* **2006**, *110*, 6073.
(40) Aloisio, S.; Francisco, J. S. *J. Phys. Chem. A* **1998**, *102*, 1899.
(41) Aloisio, S.; Francisco, J. S.; Friedl, R. R. *J. Phys. Chem. A* **2000**, *104*, 6597.

(42) Zhu, R. S.; Lin, M. C. *Chem. Phys. Lett.* **2002**, *354*, 217.
(43) Gonzalez, J.; Sucarrat,cM., T.; Anglada, J. M. *Phys. Chem. Chem. Phys.* **2010**, *12*, 2116.
(44) Long, B.; Tan, X. f.; Ren, D. S.; Zhang, W. *J. Chem. Phys. Lett* **2010**, *492*, 214.
(45) Frisch, M. J.; Trucks, G. W.; Schlegel, H. B.; Scuseria, G. E.; Robb, M. A.; Cheeseman, J. R.; Zakrzewsk, V. G.; Montgomery, J. A., Jr.; Stratmann, R. E.; Buran, J. C.; Dapprich, S.; Millam, J. M.; Daniels, A. D.; Kudin, K. N.; Strain, M. C.; Farkas, O.; Tomasi, J.; Barone, V.; Cossi, M.; Cammi, R.; Mennucci, B.; Pomelli, C.; Adamo, C.; Clifford, S.; Ochterski, J.; Petersson, G. A.; Ayala, P. Y.; Cui, Q.; Morokuma, K.; Rega, N.; Salvador, P.; Dannenberg, J. J.; Malick, D. K.; Rabuck, A. D.; Raghavachari, K.; Foresman, J. B.; Cioslowski, J.; Ortiz, V.; Baboul, A. G.; Stefanov, B. B.; Liu, G.; Liashenko, A.; Piskorz, P.; Komaromi, I.; Martin, R. G. L.; Fox, D. J.; Keith, T.; Al-Laham, M. A.; Peng, C. Y.; Nanayakkara, A.; Challacombe, M.; Gill, P. M. W.; Johnson, B.; Chen, W.; Wong, M. W.; Andres, J. L.; Gonzalez, C.; Head-Gordon, M.; Replogle, E. S.; Pople, J. A. *Gaussian 03*, revision A.01; Gaussian Inc.: Wallingford, CT, 2003.
(46) Becke, A. D. *J. Chem. Phys.* **1993**, *98*, 5648.
(47) Cremer, D.; Kraka, E.; Szalay, P. G. *Chem. Phys. Lett.* **1998**, *292*, 97.
(48) Boys, S. F.; Bernardi, F. *Mol. Phys.* **1970**, *19*, 553.
(49) Gonzalez, C.; Schlegel, H. B. *J. Phys. Chem.* **1990**, *94*, 5523.
(50) Gonzalez, C.; schlegel, H. B. *J. Phys. Chem.* **1989**, *90*, 2154.
(51) Lee, Y. S.; Kucharski, S. A.; Bartlett, R. J. *J. Chem. Phys.* **1984**, *81*, 5906.
(52) Nguyen, M. T.; Nguyen, T. L.; Ngan, V. T.; Nguyen, H. M. T. *Chem. Phys. Lett.* **2007**, *448*, 183.
(53) Lee, T. J.; Taylor, P. R.; Diag, T. *Int. J. Quantum Chem. Symp.* **1989**, *23*, 199.
(54) Rienstra-Kiracofe, J. C.; Allen, W. D.; Schaefer, H. F., III. *J. Phys. Chem. A* **2000**, *104*, 9823.
(55) Bader, R. F. W. *Chem. Rev.* **1991**, *91*, 893.
(56) Biegler-Konig, F. *J. Comput. Chem.* **2000**, *21*, 1040.
(57) Biegler-Konig, F.; Schonbohm, J.; Bayles, D. *J. Comput. Chem.* **2001**, *22*, 545.
(58) Biegler-Konig, F.; Schonbohm, J. *J. Comput. Chem.* **2002**, *23*, 1489.
(59) Eckart, C. *Phys. Rev.* **1930**, *35*, 1303.
(60) Duncan, W. T.; Bell, R. L.; Truong, T. N. *J. Comput. Chem.* **1998**, *19*, 1039.
(61) Zhang, S.; Truong, T. N. *VKLab*, version 1.0; University of Utah: Salt Lake City, UT, 2001.
(62) Cremer, D.; Gauss, J.; Kraka, E.; Stanton, J. F.; Bertlett, R. *J. Chem. Phys. Lett.* **1993**, *209*, 547.
(63) Olzmann, M.; Kraka, E.; Cremer, D.; Gutbrod, R.; Andersson, S. *J. Phys. Chem. A* **1997**, *101*, 9421.
(64) Bach, R. D.; Owensby, A. L.; Andrés, J. L.; Schlegel, H. B. *J. Am. Chem. Soc.* **1991**, *113*, 7031.
(65) Crehuet, R.; Anglada, J. M.; Cremer, D.; Bofill, J. M. *J. Phys. Chem. A* **2002**, *106* (15), 3917.
(66) Chen, B.-Z.; Anglada, J. M.; Huang, M.-B.; Kong, F. *J. Phys. Chem. A* **2002**, *106* (9), 1877.
(67) Huang, M.-B.; Chen, B.-Z.; Wang, Z.-X. *J. Phys. Chem. A* **2002**, *106* (22), 5490.
(68) Aloisio, S.; Francisco, J. S. *J. Am. Chem. Soc.* **2000**, *122*, 9196.
(69) Torrent-Sucarrat, M.; Anglada, M. J. *J. Phys. Chem. A* **2006**, *110*, 9718.
(70) Aloisio, S.; Francisco, J. S. *J. Phys. Chem. A* **1999**, *103*, 6049.
(71) Koch, U.; Popelier, P. L. A. *J. Phys. Chem.* **1995**, *99*, 9747.
(72) Anglada, J. M.; Domingo, V. M. *J. Phys. Chem. A* **2005**, *109*, 10786.
(73) Olivella, S.; Anglada, J. M.; Sole, A.; Bofill, J. M. *Chem.—Eur. J.* **2004**, *10*, 3404.
(74) Su, F.; Calvert, J. G.; Shaw, J. H. *J. Phys. Chem.* **1979**, *83*, 3185.
(75) Olivella, S.; Bofill, J. M.; Sole, A. *Chem.—Eur. J.* **2001**, *7*, 3377.
(76) Zhang, D.; Zhang, R. Y. *J. Am. Chem. Soc.* **2002**, *124*, 2692.
(77) Long, B.; Zhang, W. J.; Tan, X. F.; Long, Z. W.; Wang, Y. B.; Ren, D. S. *J. Phys. Chem. A* **2011**, *115*, 1350.
(78) (a) Iuga, C.; Alvarez-Idaboy, J. R.; Reyes, L.; Vivier-Bunge, A. *J. Phys. Chem. Lett.* **2010**, *1*, 3112. (b) Iuga, C.; Alvarez-Idaboy, J. R.; ivier-Bunge, A. *Chem. Phys. Lett.* **2010**, *501*, 11. (c) Iuga, C.; Alvarez-daboy, J. R.; Vivier-Bunge, A. *Theor. Chem. Acc.* **2011**, *129*, 209. (d) Iuga, C.; Alvarez-daboy, J. R.; Vivier-Bunge, A. *J. Phys. Chem. A* **2011**10.1021/jp201517p. (e) Uc, V. H.; Alvarez-Idaboy, J. R.; Galano, A.; Vivier-Bunge *J. Phys. Chem. A* **2008**, *112*, 7608.
(79) Hatakeyama, S.; Akimoto, H. *Res. Chem. Intermed.* **1994**, *20*, 503.
(80) Baulch, D. L.; Cox, R. A.; Hampson, R. F.; Kerr, J. A., Jr.; Troe, J.; Watson, R. T. *J. Phys. Chem. Ref. Data* **1980**, *9*, 295.
(81) Calvert, J. G.; Atkinson, R. J.; Kerr, A.; Madronich, S.; Moortgat, G. K.; Wallington, T. J.; Yarwood, G. *The Mechanisms of Atmospheric Oxidation of the Alkenes*; Oxford University Press: New York, 1999.
(82) Nazarov, A. M.; Khursan, S. L.; Kalinichenko, I. A.; Ziganshina, S. K.; Komissarov, V. D. *Kinet. Catal.* **2002**, *43*, 459.
(83) Morokuma, K.; Muguruma, C. *J. Am. Chem. Soc.* **1994**, *116* (101), 36.
(84) Steudel, R. *Angew. Chem., Int. Ed. Engl.* **1995**, *4*, 113.
(85) Loerting, T.; Liedl, K. R. *Proc. Natl. Acad. Sci. U.S.A.* **2000**, *97*, 8874.
(86) Jayne, J. T.; Poschl, U.; Chen, Y. M.; Dai, D.; Molina, L. T.; Worsnop, D. R.; Kolb, C. E.; Molina, M. J. *J. Phys. Chem. A* **1997**, *101*, 10000.
(87) Loerting, T.; Liedl, K. R. *J. Phys . Chem. A* **2001**, *105*, 5137.
(88) Derwent, R. G. Sources, Distributions and Fates of VOCs in the Atmosphere. In *Issues in Environmental Science and Technology 4, Volatile Organic Compounds in the Atmosphere*; Hester, R. E., Harrison, R. M., Eds.; The Royal Society of Chemistry: Cambridge, U.K., 1995; pp 1−17.
(89) de Gouw, J.; Warneke, C. *Mass Spectrosc. Rev* **2007**, *26*, 223.
(90) Galano, A.; Narciso-Lopez, M.; Francisco-Marquez, M. *J. Phys. Chem. A* **2010**, *114*, 5796.
(91) Zhao, J. X.; Toon, O. B; Turco, R. P. *J. Geophys. Res.* **1995**, *100*, 5215.